정전 마이크로 액츄에이터의 자동 CAE 평가
(Automated CAE Evaluation of Electrostatic Micro Actuator)

이 준성 (경기대 공대)

Joon-Seong Lee (Kyonggi Univ)

ABSTRACT

This paper describes an automated computer-aided engineering (CAE) system for micromachines whose size range 10 to 10^3 μm. An automatic finite element mesh generation technique, which is based on the fuzzy knowledge processing and computational geometry techniques, is incorporated into the system, together with one of commercial finite element (FE) analysis codes, MARC, and one of commercial solid modelers, Designbase. The system allows a geometry model of concern to be automatically converted to different FE models, depending on physical phenomena to be analyzed, i.e. electrostatic analysis, stress analysis, modal analysis and so on. The FE analysis models are then exported to the FE analysis code, and then analyses are performed. This system is successfully applied to an electrostatic micro actuator.

Key Words : Computer Aidede Engineering(CAE), Fuzzy knowledge processing(퍼지 지식처리),
Computational geometry(계산 기하학), Finite element analysis(유한요소 해석),
Micro actuator(마이크로 액츄에이터)

1. Introduction

Despite the large number of macro electrostatic actuator designs those have been proposed[1], few large-scale electrostatic actuators are in use. However, in a micro domain, an electrostatics mechanism appears to be a more advantageous to use[2] A number of efforts have been made so far to build electrostatic micro actuators[3,4]. Many of these actuators are interrelated to design and fabrication.

In accordance with dramatical progress of computer technology, numerical simulation methods such as the finite element method (FEM) are recognized to be key tools in practical designs and analyses. Computer simulations allow for the testing of new designs and for the iterative optimization of existing designs without time consuming and considerable efforts to experiments. However, conventional computational analyses of practical structures are still labour-intensive and are not easy for ordinary designers and engineers to perform.

The present author has proposed a novel automatic FE mesh generation method for three-dimensional complex geometry[5,6]. To efficiently support design processes of practical structures, this mesh generator is integrated with one of commercial FE analysis codes MARC[7] and one of commercial solid modelers Designbase[8].

The developed system is applied to evaluate one of electrostatic micro actuators[9]. Through the analyses, fundamental performances of the system are discussed.

2, Outline of the System

The developed CAE system allows designers to evaluate detailed physical behaviors of structures through some simple interactive operations to their geometry models. In other words, designers do not have to deal with mesh data when they operate the system.

2.1 Definition of geometry model

A whole analysis domain is defined using one of commercial geometry modelers, Designbase, which has abundant libraries enabling us to easily operate, modify and refer to a geometry model.

2.2 Attachment of material properties and boundary conditions to geometry model

Material properties and boundary conditions are directly attached onto the geometry model by clicking the loops or edges that are parts of the geometry using a mouse, and then by inputting actual values.

2.3 Designation of node density distributions

In the present system, nodes are first generated, and then a FE mesh is built. A node density distribution over a whole geometry model is constructed as follows. The present system stores several local node patterns such as the pattern suitable to well capture stress concentration, the pattern to subdivide a finite domain uniformly, and the pattern to subdivide a whole domain uniformly. A user selects some of those local node patterns, depending on their analysis purposes, and specifies their relative importance and where to locate them. Then a global distribution of node density over the whole analysis domain is automatically calculated through their superposition using the fuzzy knowledge processing[10]. When designers do not want any special meshing, they can adopt uniformly subdivided mesh.

2.4 Node and element generation

Node generation is one of time consuming precesses in automatic mesh generation. Here, the bucketing method[11] is adopted to generate nodes which satisfy the distribution of node density over a whole analysis domain.

The Delaunay triangulation method[12] is used to generate tetrahedral elements from numerous nodes produced within a geometry.

2.5 Attachment of material properties and boundary conditions to FE mesh

Through the interactive operations mentioned in section 2.2, a user designates material properties and boundary conditions onto parts of the geometry model. Then these are automatically attached onto appropriate nodes, edges, faces and volume of elements. Such automatic conversion can be performed owing to the special data structure of finite elements such that each part of element knows which geometry part it belongs to. Finally, a complete FE model consisting of mesh, material properties and boundary conditions is created.

2.6 FE analyses

The present system automatically converts geometry models of concern to various FE models, depending on physical phenomena to be analyzed, i.e. stress analysis, eigen value analysis, thermal conduction analysis, electrostatic analysis, and so on. The current version of the system produces FE models of quadratic tetrahedral elements, which are compatible to one of commercial FE codes, MARC. FE analyses are automatically performed. FE models and analysis results are visualized using a pre/post processor of MARC, MENTAT[7].

3. Electrostatic Micro Actuator

The micro actuator considered in the present study is designed as a part of a highly accurate positioning device[13]. This actuator uses an electrostatic force as other micro-motors do, and its fabrication process is almost the same as those in ref.[14].

Materials employed here are silicon and silicon compounds, which are well known as materials for semiconductor devices.

The basic structure of the present actuator is illustrated in Fig. 1. Fig. 1(a) is its schematic plane view, and Fig. 1(b) its cross-section view.

The micro actuator comprises a movable plane ring, i.e. rotor, three spiral beams, and a plurality of electrodes, i.e. stators. Dimensions of its reference design are as follows. The platform is a ring-like plate of approximately 200 μm in outer diameter and 150 μm in inner diameter.
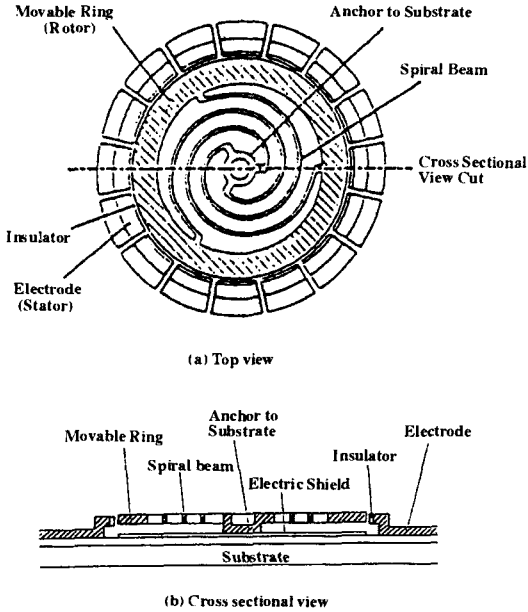

(a) Top view

(b) Cross sectional view

Fig. 1 Basic structure of micro actuator

The three beams are disposed at the inner space of the ring, and connect the ring with the substrate. The electrodes are placed in the circumferential direction around the ring. The inner diameter of a set of the electrodes is by 3 μm larger than the outer diameter of the ring. As each electrode is excited sequentially, the driving force produced as an electrostatic attraction force is generated between the ring and one of the electrodes, and the ring rolls along the inside surface of the electrodes with a little distortion of the three spiral beams. When the ring rolls one cycle without slipping, it has transversed a distance of the circumference of the inner surface of the electrodes subtracted by its own circumference. Although the rotation of the ring is limited due to the spiral beams, the present actuator has several advantages including high torque and low friction. This electrostatic micro

actuator is to be used as a micro-positioner. Reference dimensions of the actuator are shown in Table 1. Material properties are summarized in Table 2.

Table 1 Reference dimensions

Diameter of Plane Ring	200 μm
Thickness of Plane Ring	2.5 μm
Inner Diameter of Electrodes	206 μm
Width of Spiral Beams	5.0 μm
Thickness of Spiral Beams	2.5 μm
Thickness of Insulator	1.0 μm

Table 2 Material properties

Material	Si
Young's Modulus	190 GPa
Poisson's Ratio	0.3
Yield Stress	7 GPa
Mass Density	2300 kg/m³
Permittivity of Insulator	4.0

4. Results and Discussions

To compare with solutions of the three-dimensional(3D) electrostatic FE analyses, the analytical 2D calculation of the torque generated by the electrostatic micro actuator is performed.

4.1 Theoretical analysis of starting torque

A sketch of the rotor (ring) and stator (electrode) is shown in Fig. 2. The width of the electrode is w and subtends an angle of θ_s to θ_c at the center of the stator. As shown in figure, the radius of the rotor id r_r, the radius of the stator is r_s, and the angular position of the electrode center is θ. In this figure, the rotor has been moved to the right until it touches an insulating layer of thickness t_i on the stator. The gap between the rotor and stator is filled with an insulator, and the rest is filled with air. If the relative permittivity of the insulator is ε_i, then the effective distance between the rotor and stator, d_E, can be calculated.

$$d_E = d - t_i\left(\frac{\varepsilon_i - 1}{\varepsilon_i}\right) \qquad (1)$$

where d is a distance between the rotor and stator, and can be defined d(θ). Considering this function d(θ) is varied from d_s to d_e, the potential energy stored in the gap is expressed as below.

$$U = \int_{\theta_i}^{\theta_r} dU = \int_{\theta_i}^{\theta_r} \frac{\varepsilon_0 t \, V^2 \, r_s}{2 d_E} d\theta \qquad (2)$$

where ε_0 is the dielectric constant of the vacuum, t is the thickness of the plane ring and V is the applied voltage to the electrodes.
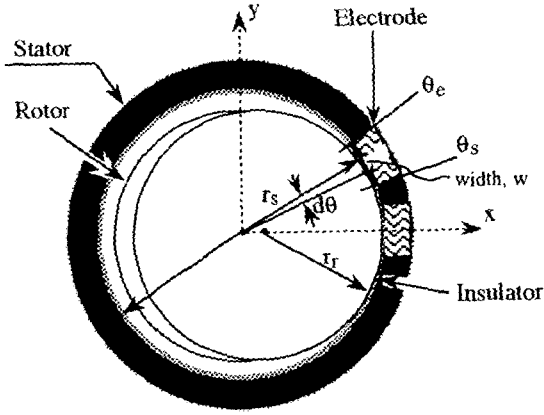

Fig. 2 A diagram of the rotor and stator

There are two different angles associated with this motor as shown in Fig. 3. The angle ϕ is the angle of rotation of the rotor, and the θ is the angle to the energized electrode. That is, the distance from the electrode A to B is the same distance from C to D of the rotor by the contact point. The ratio of θ to ϕ is given as follows :

$$r_r(\theta + \phi) = r_s \theta \qquad (3)$$

$$\frac{\theta}{\phi} = \frac{r_r}{r_s - r_r} \qquad (4)$$

The torque can be expressed as follows ;

$$= \frac{dU}{d\phi} = \frac{dU}{d\theta} \cdot \frac{d\theta}{d\phi} = \frac{dU}{d\theta} \cdot \frac{r_r}{r_s - r_r}$$

$$= \left[\frac{r_r}{r_s - r_r} \right] \frac{d}{d\theta} \left[\frac{\varepsilon_0 t \, V^2 \, r_s}{2} \right] \int_{\theta_i}^{\theta_r} \frac{1}{d_E} d\theta$$

$$\left[\frac{r_r}{r_s - r_r} \right] \left[\frac{\varepsilon_0 t V^2 r_s}{2} \right] \left(\frac{1}{d_E} \Big|_{\theta_r} - \frac{1}{d_E} \Big|_{\theta_i} \right) \qquad (5)$$

Considering the insulator, the starting torque is eventually calculated as follows :

$$\tau = \left[\frac{r_r}{(r_r - t_i) - r_r} \right] \left[\frac{\varepsilon_0 t V^2 r_r}{2} \right] \left(\frac{1}{d_E} \Big|_{\theta_r} - \frac{1}{d_E} \Big|_{\theta_i} \right) \qquad (6)$$
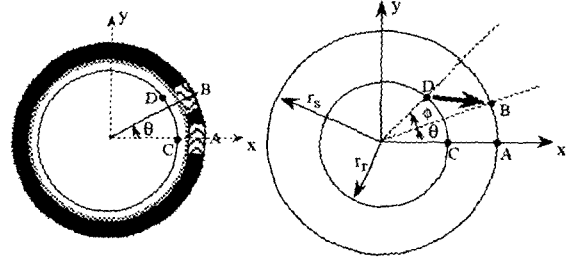

Fig. 3 Motion of motor

4.2 FE analyses results

Using an automated analysis system, the in-plane deformation analysis of the ring with the spiral beams caused due to an electrostatic force and electrostatic analysis of the air gap between the ring and one of the electrodes.

4.2.1 In-plane deformation of ring with beams

Assuming the reference dimensions of the rotor listed in Table 1, its in-plane deformation is analyzed to evaluate the quantitative relationship between a rotation angle and a torque necessary to rotate the rotor within the elastic limit of the beams.

Fig. 4 shows the relationship between the calculated torque τ_s and the rotation angle. It can be seen from the figure that the rotation angle of the rotor is limited at about 62 degrees because of the elastic limit. Fig. 4 also tells us that the starting torque required is 0.42×10^9 Nm. This value will be referred to in the section of electrostatic analyses.

4.2.2 Electrostatic analysis

To estimate electrostatic performances of micro

actuators, in-plane two-dimensional FE analyses are often performed because of complexity of actual micro actuator geometry. Here, an actual 3D geometry of the micro actuator are considered. Fig. 5 shows a geometry model and boundary conditions of part of the air gap between the rotor and the stators. Here a sufficiently large area of the air is modeled in order to approximately take into account infinite boundary conditions.
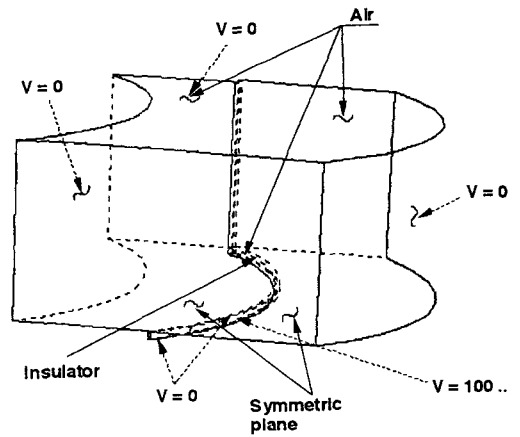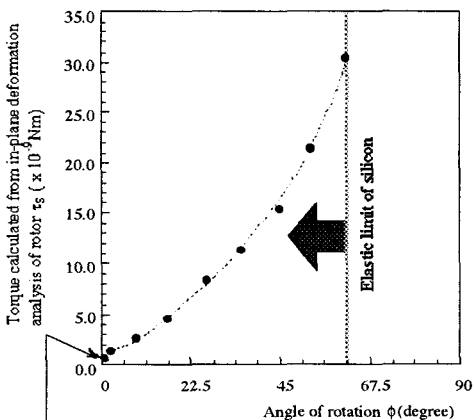
When one of the electrodes is excited, the rotor is electrostatically attracted, and comes to contact with the insulator on the inner surface of the electrode. When the next electrode is excited, the rotor revolves without slipping. Fig. 6 shows a calculated starting torque τ_e vs. driving voltage curves. The solid curve denotes the 3D FE solution, while the broken curve does the 2D analytical one. It can be seen from this figure that the starting torque is proportional to the square of driving voltage, and that the 2D analytical solution is four to five times larger than the 3D FE one. Such a significant difference may be caused due to the omit of electrical leakage in the 2D analytical solution. Considering that the torque of 0.42×10^{-9} Nm is necessary to start rotating the rotor as given in section 4.2.1, it is obvious from Fig. 6 that a driving voltage exceeding 170 V is indispensable.

Fig. 5 Geometry model and boundary conditions for air gap between rotor and one of stators
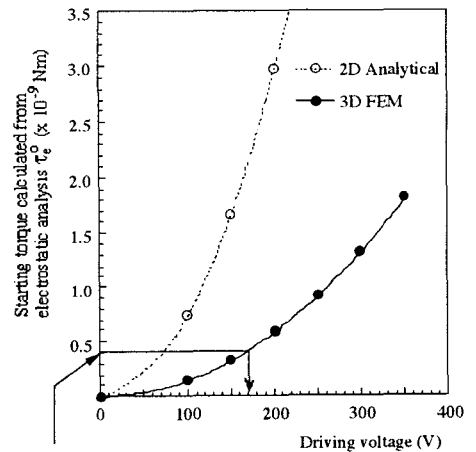
Required starting torque
$\tau_s^o = 0.42 \times 10^{-9}$ Nm

Fig. 6 Calculated starting torque vs. driving force

Starting torque : $\tau_s^o = 0.42 \times 10^{-9}$Nm

Fig. 4 Calculated torque vs. rotation angle

5. Conclusions

An automated analysis system for micro actuator is developed in the present study. Interactive operations to be done by a user are performed in a reasonably short time even when solving complicated problems such as micro actuators. The other processes which are time consuming and labour-intensive in conventional systems are fully automatically performed in a popular engineering workstation environment. This system is successfully applied to the evaluation of performances of an electrostatic micro actuator.

References
[Omit]